Research on Uplift Bearing Performance of Assembled Steel Pipe Pile used in Transmission Lines in Mountainous Terrain

Kun Zhou[1], *Linhua Chen*[1], *Xiangyu* Gu[2], *Qi* Zhang[2]

[1]Economy and Technology Research Institute, State Grid Hunan Electric Power Company, Changsha, Hunan, 410004, China

[2]School of Civil Engineering, Southeast University, Nanjing, Jiangsu, 211100, China

Corresponding author: Dr. Zhang Qi, 34266513@qq.com

Abstract : Assembled steel pipe pile, which is a novel pile foundation, is developed in the paper. The ultimate uplift bearing capacity of the pile is proposed, and simulation by Plaxis3D and the corresponding experiment are performed to verify the theory. In the simulation, ultimate uplift bearing capacity of the assembled steel pipe pile and ultimate lateral frictional resistance of the interface of pile-soil increases with the increasing of the strength and stiffness of the interface of pile-soil, and with the increasing of length-diameter ratio, ultimate uplift bearing capacity of the assembled steel pipe pile increases while the ultimate lateral frictional resistance decreases gradually. The ultimate lateral friction is influenced by both of the strength of the soil around the pile and the interface of pile-soil, and the ultimate uplift bearing capacity obtained by simulation and theoretical calculation are close. Long-gauge FBG sensors are used in the experiment for measuring the longitudinal strain of the pile, and the error of ultimate uplift bearing capacity between the results of experiment and theory is less than 10%.

Key words : assembled steel pipe pile; ultimate uplift bearing capacity; frictional resistance; finite element analysis; long-gauge FBG sensors

1.Introduction

With the development of the social economy, the construction of electrical engineering is becoming increasingly important. As an important part of the construction of electrical engineering, transmission line engineering has the properties that the line is long, the region is wide, and the conditions of topography, geomorphology and hydrology are complex. The restricting factors of the line corridors such as the lack of land resources, environmental protection leads that the line inevitably go through the hills or mountains which are steep and inconvenient to transport. According to statistics, the foundation construction of transmission line accounts for more than 60% of the construction period, so the foundation construction in mountainous terrain is the most primary factor for restricting the construction period.

At present, most piles used in the foundation construction of transmission engineering in mountainous terrain are bored concrete piles and the production of concrete is in the spot, which consumes lots of manpower and material resources to transport the sand, cement, water and other materials. Compared with the bored concrete pile, steel pipe pile has the advantages of high stiffness, strong ability for resisting the moment and shear, short construction period, and convenient to accomplish, which is widely used in the world since the 1950s. Although the steel pipe pile is convenient to construction in the spot, the diameter and length of the pile is usually large which leads that the transportation of it is inconvenient in mountainous terrain. The assembled structure is convenient to transport and has high production efficiency compared with the integral structure. Combined with the advantages of the steel pipe pile, a novel foundation form of transmission line is proposed as assembled steel pipe pile foundation. Because the top of the pile foundation of transmission line bears the horizontal and vertical load from

the superstructure and the uplift bearing capacity is the control condition for designing the foundation of transmission line [1], the uplift bearing capacity of the assembled steel pipe pile is need to be researched.

In the research about uplift bearing capacity of the pile foundation, Chattopadhyay et al.[2] proposed a method for predicting ultimate uplift bearing capacity of the pile foundation in sand by considering the diameter, length and surface of the pile and the character of the soil. Deshmukh et al.[3] established the relation between critical depth ratio of the pile and ultimate uplift bearing capacity in the cohesionless soil and the predicted results are compared with the experiment data. Khatri et al.[4] studied the ultimate uplift bearing capacity of the pile under the vertical load based on the hypothesis that the cohesive force of the cohesive soil increases linearly with increasing of the depth on the undrained condition. Shanker et al.[5] developed a semi-empirical model for predicting the ultimate uplift bearing capacity of the pile in the sand and it is verified by the experiment. Alawneh et al.[6] studied the influence factors about the ultimate uplift bearing capacity of the pile in the dry sand. Shelke et al.[7] modified the lateral soil pressure coefficient by considering the soil arch effect and the modified method is verified by the test. Zhu et al.[8] deduced the elastic solution about the uplift pile based on winkler foundation model and researched the deformation and bearing capacity of the pile. Huang et al.[9] proposed an uniform method for calculating the bearing capacity about different pile length based on finite element modelling. Qian et al.[10] studied the deformation characteristics of the pile through the shear test and numerical analysis. Yu et al.[11] simulated the process of uplifting the large diameter rotary excavated filling pile and the corresponding experiment results are compared to analyze the internal force of the pile.

The researches about bearing capacity of the uplift pile are mainly focus on the filling pile, while the studies about the steel pipe pile on this aspect are less, and the corresponding researches of the assembled steel pipe pile are little. In this paper, the structure of the foundation of assembled steel pipe pile is presented firstly in section 2.

2 The structure of assembled steel pipe pile

The structure of the pile body in the foundation of assembled steel pipe pile, which is composed of grouting, steel pipe and the filling soil in the pile, is strikingly different from the traditional digging pile. The construction process of the assembled steel pipe pile mainly contains precasting of the pile, installation in the spot, and pressure grouting. Firstly, the pile is precasted in the factory or spot according to the desired size. And then, the pile is put in the foundation pit by sections. At last, the grouting is grouted for filling the gap between the pit wall and the pile body.

The foundation of assembled steel pipe pile is mainly composed of pyramid stents, precasted steel pipe and connection fittings. The steel pipe is connected to the steel tower by pyramid stents, and the steel pipes are connected with each other by flanges. The sketch of the foundation of assembled steel pipe pile is shown in Figure 1.

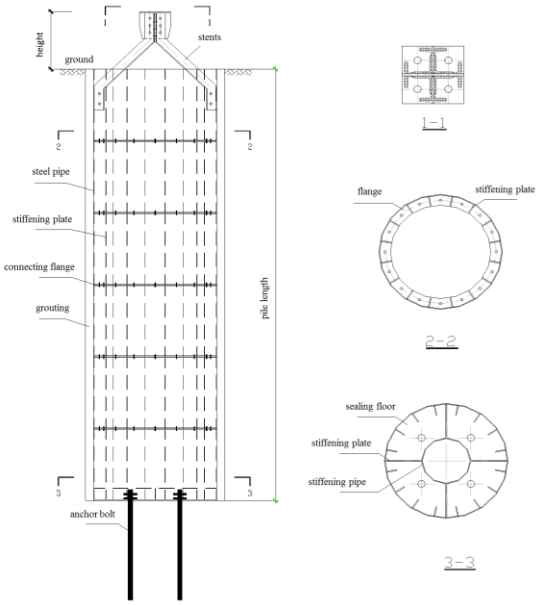

(a) Sketch of the assembled steel pipe pile

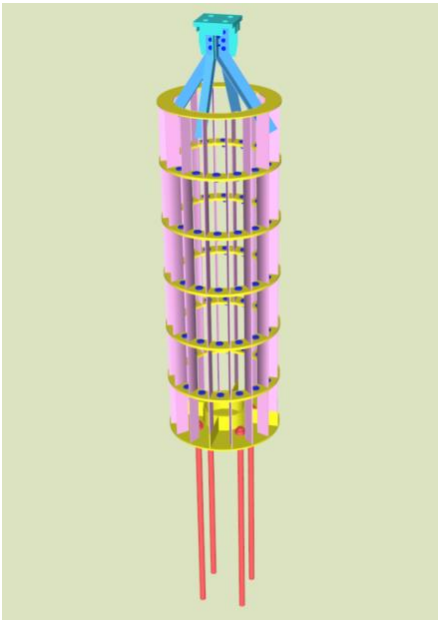

(b) Rendering of the assembled steel pipe pile

Fig.1 Assembled steel pipe pile

The top of the pyramid stents is connected to the tower foot by a thick plate, and the large diameter bolts are used to fix the thick plate and tower foot. The bottom of the pyramid stents is connected to the stiffening plate of the steel pipe by angle iron. As for the precasted steel pipe, it is divided to the top, middle and bottom parts by position. The middle part is connected to the top and bottom ones by flange and stiffening plate. The bolt holes at stiffening plate of the top part are reserved for connecting to the steel support. And the closed flat shape is adopted to the bottom part for welding the steel plate in the bottom. The connection fittings of the pipe include thick plate, cross plate, bolt, nut, gasket and so on. If the medium or weakly weathered rocks are under the cladding, the combination of the foundations of assembled steel pipe pile and rock anchor can be adopted. In this syncretic foundations, the steel pipe pile is subjected to the pressure, horizontal force and partial uplift force and the rock anchor is subjected to the residual uplift force. The syncretic foundations take advantages of both superiorities of the foundations of assembled steel pipe pile and rock anchor, and the corresponding construction period is short with low cost.

3 Ultimate uplift bearing capacity of the assembled steel pipe pile

The main factors for influencing the ultimate uplift bearing capacity contain length and diameter of the pile, property of the soil around the pile, interface property between pile and soil and the size of anchor. Considering the weight of assembled steel pipe pile and the inner soil, the ultimate uplift bearing capacity of the assembled steel pipe pile can be expressed as

$$Q_{uk} = U\sum_{i=1}\alpha_i q_{sik} l_i + G_p + \xi f u_r h_r \quad (1)$$

where U is the pile girth, q_{sik} and α_i are the interface ultimate friction and the corresponding correction coefficient about the ith layer of the soil respectively, l_i is the thickness of ith layer of the soil, G_p is the weight of assembled steel pipe pile and the inner soil, ξ is the empirical coefficient, which is 0.8 for the permanent anchor and 1 for the temporary one, u_r is the girth of the anchor, h_r is the length of the embedded section of the anchor, and f is the characteristic value of bonding strength between mortar and rock, which can be set according to the GB 50007-2011 [12].

In equation (1), the parameters can be set according to the engineering experience except α_i. As the result that the pile side frictional resistance is influenced by pile-soil interface strength and soil strength, it need to modify the pile-soil interface strength for obtaining the real value of the pile side friction.

4. Analysis based on finite element

4.1 Engineering background and geometric model

The transmission line engineering of 220 kV between Yongzhou and Linwu in Hunan is from Lanshan 220 kv substation to Linwu 220 kv substation. The line length of the proposed project is about 52.8km, and the topography along the line is cragged. The main topography is low-hilly, whose elevation ranges from 300m to 500m.

Plaxis3D is used for simulating the assembled steel pipe pile in this paper as shown in Figure 2, and the influences about different grouting conditions on the ultimate bearing capacity of the pile is researched. In the simulated model, the length of steel pipe pile is 10m, and the pile is established by 10 sections, whose outer diameter is 1m and thickness is 0.01m. The displacement of the bottom of the pile is fixed, the lateral displacement of the pile side is fixed while the vertical displacement is free, and the displacement of top surface of the pile is free. The three dimensions of the whole model in Figure 2 are 20m. According to the practical engineering, the material property parameters of the finite element is list in Table 1. The soil with the depth ranges from 0 to 3m is hard plastic clay and the soil with the depth exceeds 3m is decomposed rock.

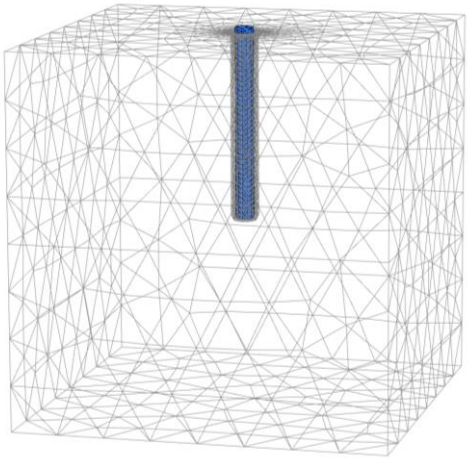

Fig. 2 Finite element model of assembled steel pipe pile

Table 1 Material Property Parameters

Material	γ (kN·m^{-3})	E (MPa)	ν	c (kN·m^{-2})	φ (°)
hard plastic clay	20	250	0.4	30	22
decomposed rock	22.5	1300	0.35	200	27

steel pipe pile	78.5	206000	0.3
grouting	20	28000	0.18

4.2 Constitutive relation and hypothesis

The strengths of pile and grouting are greater than the soil, so they seldom be strength-broken. The pile and grouting are simulated by linear elastic model, and they are regarded as a whole with assuming that the interface will not be damaged. The 10-node Mohr-Coulomb model is adopted to simulate the soil, and the yield criterion of Mohr-Coulomb is used. The elasto-plastic Coulomb friction model is adopted as the contact model between pile and soil, which is shown in Figure 3.

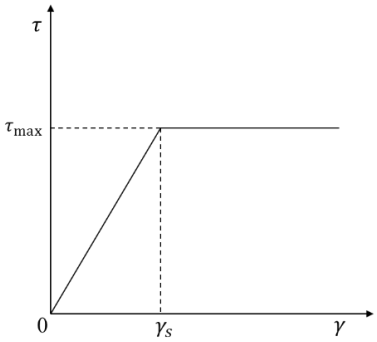

Fig 3 Elastic-plastic coulomb friction model

4.3 Analysis of the characteristic about uplift bearing capacity

Load incremental finite element method is used in the simulation. The vertical uplifting load is applied on the top of the pile, and the load-displacement curve of the top of the assembled steel pipe pile is obtained as shown in Figure 4. When the uplifting load is low, the load-displacement curve is linear. While when the uplifting load reaches 5025kN, the inflection point A appears in the figure, which indicates that the ultimate uplift bearing capacity is 5025kN in this condition.

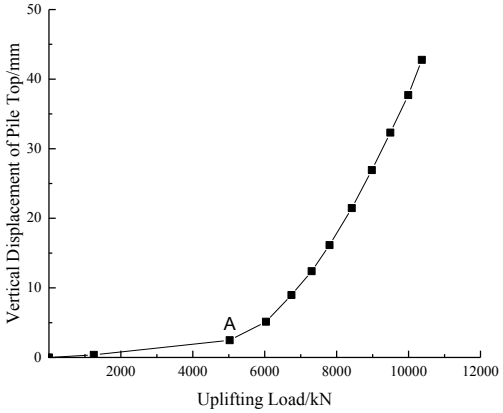

Fig. 4 Load-displacement curve of the top of the assembled steel pipe pile

Relative shear stress contours about two values of P are shown in Figure 5. In Figure 5(a), the relative shear stress of hard plastic clay with depth 0-3m reaches to 1 firstly, which indicates that the soil around the pile is in plastic state at this time. When the applied load reaches to the ultimate uplift bearing capacity which is 5025kN, the plastic zone of hard plastic clay expends and relative shear stress of the decomposed rock around the pile increases but don't reach the plastic state as shown in Figure 5(b).

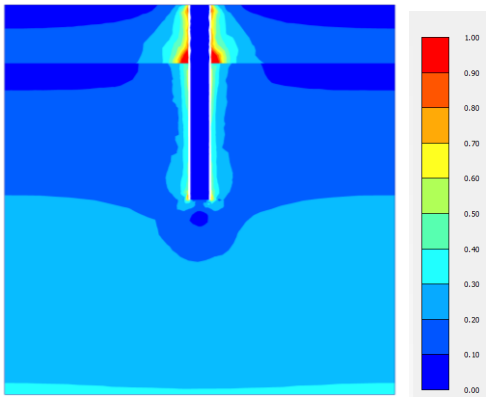

(a) P=4086 kN

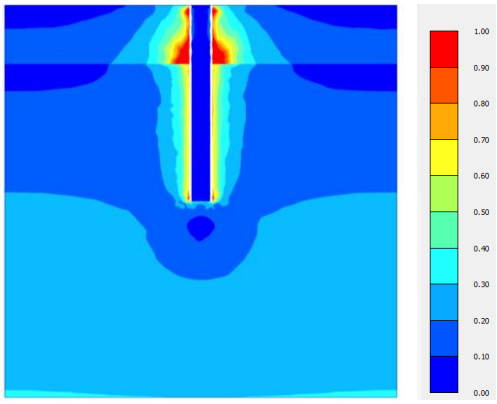

(b) P=5025 kN

Fig. 5 Relative shear stress contours of the soil around the pile

Figure 6 shows the relative shear stress contours of pile-soil contact surface. In the figure, it can be found that when the load P reaches 4086kN, interface of pile-soil with depth 0-3m reaches plastic state and the region with depth larger than 3m is in the elastic state. When the load P reaches 5025kN, the whole interface of pile-soil reaches plastic state. According to Figures 5 and 6, when the pile reaches the ultimate uplift bearing capacity, the soil and interface from the layer of hard plastic clay reaches plastic state, and the rock from the layer of decomposed rock is in the elastic state while the interface from the same layer reaches

plastic state.

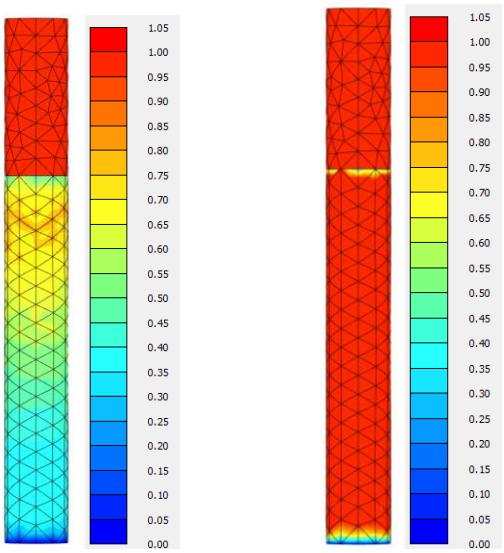

(a) P=4086kN (b) P=5025kN

Fig. 6 Relative shear stress contours of pile-soil contact surface

4.4 Parametric analysis

In order to study the influence of grouting condition and length-diameter ratio on the uplift bearing capacity, the finite element simulation is used to analyse.

Because the grouting condition influences the strength and stiffness of the interface of pile-soil, different values of strength and stiffness are adopted for simulating the different grouting condition. In the paper, four groups of value are included and the corresponding parameters are shown in Table 2. The curve of load-displacement of the pile obtained by simulation is shown in Figure 7.

Table 2 Ultimate uplift bearing capacity of the pile at different strength and stiffness of the pile-soil interface

Group	Soil type	G (kN·m^{-2})	Es (kN·m^{-2})	c (KPa)	φ (°)	P_u (kN)
1	hard plastic clay	32144	353590	18	13.6	4234
	decomposed rock	173340	1906700	120	17.0	
2	hard plastic clay	43752.1	481270	21	15.8	5025
	decomposed rock	235935	2595300	140	19.6	
3	hard plastic clay	57146	628600	24	17.9	6315
	decomposed rock	30816	3389800	160	22.2	
4	hard plastic clay	72324.9	795570	27	20.0	7124
	decomposed rock	390015	4290200	180	24.6	

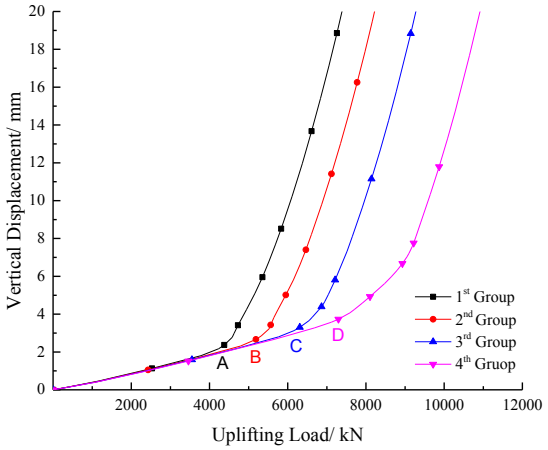

Fig. 7 Load-displacement curve about different grouting conditions

There are obvious inflection points A, B, C and D in Figure 7, which are correspond to the ultimate uplift bearing capacity about the different conditions. When the uplift loading exceeds the bearing capacity, the displacement of the top of pile increases rapidly. In Table 2, the bearing capacity of the 4th group is 7124 kN, which is the minimum, while the value of the 1st group is 4234 kN, which is the maximum. The results show that the ultimate uplift bearing capacity of the assembled steel pipe pile increases with the increasing of the strength and stiffness of the interface of pile-soil.

Ultimate lateral frictional resistance of the pile with different depths are shown in Figure 8. Ultimate lateral frictional resistance of the interface of pile-soil increases with the increasing of the strength and stiffness of the interface of pile-soil. Because the property of the soil changes at the depth 3m, ultimate lateral frictional resistance increases suddenly at the depth 3m and the uplift bearing capacity of the pile increases largely. The distribution of lateral friction is parabolic profile.

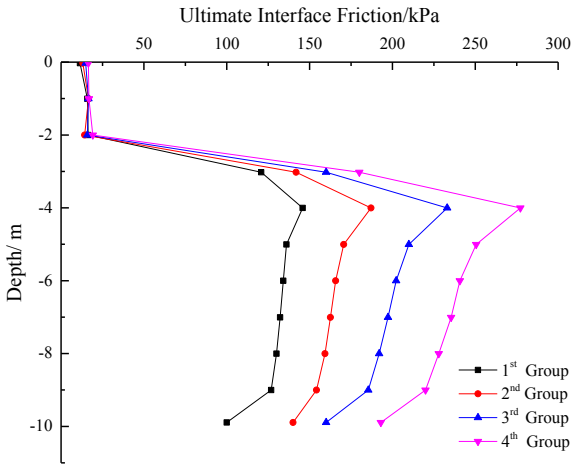

Fig. 8 Ultimate interface friction distribution curves about different groups

In the same grouting condition and lateral area, the influence of different length-diameter ratio on the ultimate uplift bearing capacity of the assembled steel pipe pile is studied. The length-diameter ratios are set 27.778, 15.625, 10.000, 6.944 respectively for simulation. The curve of load-displacement of the top of pile is obtained as Figure 9 and the corresponding results are list in Table 3.

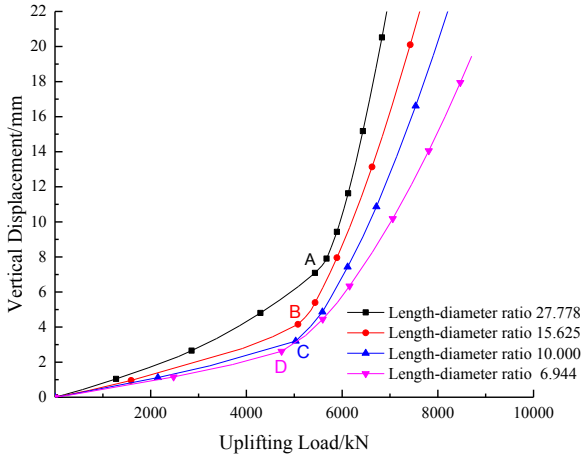

Fig. 9 Load-displacement curve about different length-diameter ratios

Table 3 Ultimate uplift bearing capacity of the pile at different length-diameter ratios

Lateral area of the pile (m^2)	D (m)	L (m)	L (D)	P_u (kN)
10	0.6	16.667	27.778	5696
	0.8	12.500	15.625	5226
	1.0	10.000	10.000	5025
	1.2	8.333	6.944	4734

In Figure 9, the displacement increases quickly after the load exceeds the critical value. From Table 3, the maximum of bearing capacity is 5696 kN when the length-diameter ratio is 16.667 and the minimum value is 4734 kN with the length-diameter ratio 8.333. In the condition of same lateral area, the embedded depth of the pile in the decomposed rock increases with the decreasing of the pile diameter, which lead to that the bearing capacity increases. As shown in Figure 10, when the pile reaches to the ultimate uplift bearing capacity, the lateral frictional resistance of the interface increases firstly and then decreases in the condition that the length-diameter ratio is different. And with the increasing of length-diameter ratio, lateral frictional resistance of the interface decreases gradually.

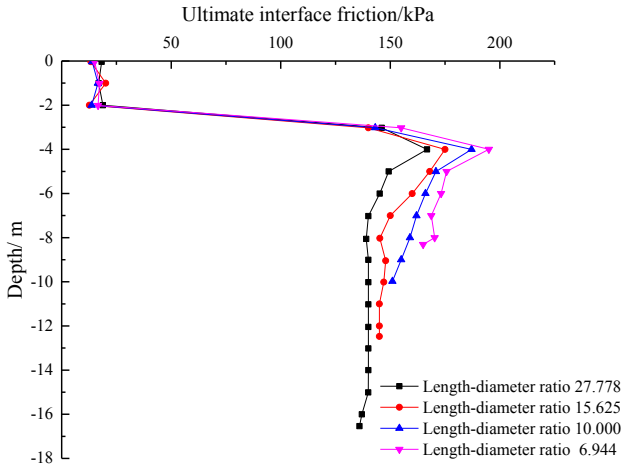

Fig. 10 Ultimate interface friction distribution curves about different length-diameter ratios

4.5 Ultimate uplift bearing capacity of the simulated pile

According to equation (1), the ultimate uplift bearing capacity of the assembled steel pipe pile mentioned in the section 4.1 can be expressed as

$$Q_{uk} = U(\alpha_1 q_{s1k} l_1 + \alpha_2 q_{s2k} l_2) + G_p \quad (2)$$

where Q_{uk} is the ultimate uplift bearing capacity of single pile, α_1 and α_2 are the interface ultimate frictional resistance correction coefficients of hard plastic clay and decomposed rock. The least square method is used to fit the correction coefficients according to the results in the simulation under different grouting conditions and the correction coefficients are list in Table 4. Then the fit coefficients are used to predict the ultimate uplift bearing capacity of a group of piles. The predicted results are compared with the finite element as shown in Table 5.

Table 4 Correction coefficients of the interface

Grouting condition	q_{s1} (kPa)	q_{s2} (kPa)	P_u (kN)	α_1	α_2
1	15.611	132.013	4234	0.908	1.31
2	16.839	165.048	5025		
3	18.222	200.303	6315		
4	20.038	234.310	7124		

(*Note*: q_{s1} is for hard plastic clay and q_{s2} is for decomposed rock)

Table 5 Comparison of the predicted and practical bearing

capacities

L/*D*	q_{s1} (kPa)	q_{s2} (kPa)	P_{u1} (kN)	P_{u2} (kN)	error (%)
27.778	16.975	145.181	5178	5696	9.09
15.625	17.452	150.116	5036	5226	3.62
10.000	16.839	165.048	5152	5025	2.53
6.944	16.810	168.280	4891	4734	3.31

(*Note*: P_{u1} is the predicted bearing capacity and P_{u2} is the practical bearing capacity)

In Table 5, the error is less than 10%, which indicates that the formula of ultimate uplift bearing capacity of the assembled steel pipe pile is reliable.

5 Experiment about the assembled steel pipe pile

The experiment is for testing the uplift bearing capacity of the assembled steel pipe pile at different grouting pressures. The geometric similarity ratio is 1:10 in the scale experiment, and the elastic modulus is consistent with the original structure. The used soil is field remolded, and the rock is strongly weathered sandstone. The box for filling the soil is 1m wide, 1m long, and 1.3m high. Long-gauge FBG sensors are used in the experiment, which can coverage the region of interest, for measuring the longitudinal strain of the assembled steel pipe pile. The deployment of the Long-gauge FBG sensors are shown in Figure 11. Each segment of FBG is 0.1m long, and 16 segments are used in the experiment. The length of pile is 1.1m long, and 8 sensors are deployed at each side of the pile for measuring the longitudinal strain and stress. The corresponding mean strain of the measuring point is expressed as

$$\varepsilon_{Ni} = \frac{\varepsilon_{FBGi}+\varepsilon_{FBGi}'}{2} \tag{3}$$

where ε_{Ni} is the mean strain of i^{th} measuring point, ε_{FBGi} and ε_{FBGi}' are the measured strains by the long-gauge FBG sensors at the two sides of the i^{th} measuring point. The longitudinal stress of the pile is shown as

$$F_i = A_P E_P \varepsilon_{Ni} = \frac{(D_o^2-D_i^2)\pi}{4} E_P \varepsilon_{Ni} \tag{4}$$

where D_O and D_i are the outer and inner diameters of the pile, and E_P is the elasticity modulus of the pile. The plastic clay and decomposed rock with depth 1.1m are researched in the experiment. The MTS servo loading system is applied as shown in Figure 12.

Fig. 11 The deployment of the Long-gauge FBG sensors

Fig. 12 Loading on the steel pipe pile

In the results of the experiment, the maximum uplift load about plastic clay obtained by the MTS is 2244N, and the maximum longitudinal load calculated by long-gauge FBG sensors is 2079.6N. As for the decomposed rock the maximum uplift load is 4782N, and the maximum longitudinal load is 4735.9N. The errors between the experiment result and theoretical value from equation (1) are less than 10%.

6 Conclusion

The conclusions of the paper are summarized as (1) Ultimate uplift bearing capacity of the assembled steel pipe pile and ultimate lateral frictional resistance of the interface of pile-soil increases with the increasing of the strength and stiffness of the interface of pile-soil, and with the increasing of length-diameter ratio, ultimate uplift bearing capacity of the assembled steel pipe pile increases while the ultimate lateral frictional resistance decreases gradually; (2) When the assembled steel pipe pile reaches to the ultimate uplift bearing capacity, the distribution of lateral frictional resistance is parabolic profile; (3) The ultimate lateral friction is influenced by both of the strength of the soil around the pile and the interface of pile-soil, and the ultimate uplift bearing capacity obtained by simulation and theoretical calculation are close; (4) The theoretical value of the ultimate uplift bearing capacity is verified by the experiment, and the

errors are less than 10%, which indicates that the theory is reliable. In the future, the influence of more parameters such as the grouting pressure, water-cement ratio and concrete age on the bearing capacity is need to research.

References

[1] ASCE 74-2009**,**Guidelines for Electrical Transmission Line Structural Loading [S]. Reston: American Society of Civil Engineers, 2009.

[2] Chattopadhyay B C, Pise P J. Uplift Capacity of Piles in Sand[J]. Journal of Geotechnical Engineering, 1986, 112(9):888-904.

[3] Deshmukh V B, Dewaikar D M, Choudhury D. Computations of uplift capacity of pile anchors in cohesionless soil[J]. Acta Geotechnica, 2010, 5(2):87-94.

[4] Khatri V N, Kumar J. Uplift Capacity of Axially Loaded Piles in Clays[J]. International Journal of Geomechanics, 2011, 11(1):23-28.

[5] Shanker K, Basudhar P K, Patra N R. Uplift capacity of single piles: predictions and performance[J]. Geotechnical & Geological Engineering, 2007, 25(2):151-161.

[6] Alawneh A S, Malkawi A I H, Aldeeky H. Tension tests on smooth and rough model piles in dry sand[J]. Canadian Geotechnical Journal, 2011, 36(4):746-753.

[7] Shelke A, Mishra S. Uplift Capacity of Single Bent Pile and Pile Group Considering Arching Effects in Sand[J]. Geotechnical & Geological Engineering, 2010, 28(4):337-347.

[8] ZHU Bi-tang, YANG Min. Calculation of displacement and ultimate uplift capacity of tension piles[J]. Journal of Building Structures, 2006, 27(3):120-129.

[9] HUANG Mao- song, WANG Xiang-jun, WU Jiang-Bin, et al. Unified approach to estimate ultimate bearing capacity of uplift piles with enlarged base[J]. Chinese Journal of Geotechnical Engineering, 2011, 33(1):63-69.

[10] QIAN Jiang-gu, MA Xiao, Li Wei-wei, et al. Centrifuge model test and in-site observation on behaviors of side-grouting uplift pile[J]. Yantu Lixue/rock & Soil Mechanics, 2014, 35(5):1241-1246+1254.

[11] YU Dan, DU Peng-xiang, ZHANG Hai-yang, et al. Numerical Simulation and Experimental Study on Bearing Behaviors of Single Tension Pile[J]. Journal of Shenyang Jianzhu University, 2014, 30(5):818-825.

[12] GB 50007-2011 Code for design of building foundation[S]. Beijing: China Architecture & Building Press,2011.